

## FRIB CRYOMODULE DESIGN AND PRODUCTION\*

T. Xu<sup>†</sup>, H. Ao, B. Bird, N. Bultman, E. Burkhardt, F. Casagrande, C. Compton, J. Crisp, K. Davidson, K. Elliott, A. Facco<sup>1</sup>, R. Ganni, A. Ganshyn, W. Hartung, M. Ikegami, P. Knudsen, S. Lidia, I. Malloch, S. Miller, D. Morris, P. Ostroumov, M. Reaume, J. Popielarski, L. Popielarski, M. Shuptar, S. Shanab, G. Shen, S. Stark, K. Saito, J. Wei, J. Wenstrom, M. Xu, Y. Xu, Y. Yamazaki and Z. Zheng, Facility for Rare Isotope Beams, Michigan State University, East Lansing, MI, USA  
 M. Wiseman, Thomas Jefferson National Accelerator Facility, Newport News, VA, USA  
 M. Kelly, Argonne National Laboratory, Lemont, IL, USA  
 R. Laxdal, TRIUMF, Vancouver, Canada  
 K. Hosoyama, High Energy Accelerator Research Organisation, Tsukuba, Japan  
<sup>1</sup>also at INFN - Laboratori Nazionali di Legnaro, Legnaro (Padova), Italy

### Abstract

The Facility for Rare Isotope Beams (FRIB), under construction at Michigan State University, will utilize a driver linac to accelerate stable ion beams from protons to uranium up to energies of >200 MeV per nucleon with a beam power of up to 400 kW. Superconducting technology is widely used in the FRIB project, including the ion sources, linac, and experiment facilities. The FRIB linac consists of 48 cryomodules containing a total of 332 superconducting radio-frequency (SRF) resonators and 69 superconducting solenoids. We report on the design and the construction of FRIB cryomodules.

### INTRODUCTION

The Facility for Rare Isotope Beams (FRIB) at Michigan State University (MSU) will advance the frontier of heavy-ion beam power by two orders of magnitude compared to existing accelerators when it reaches its design beam power of 400 kW [1]. In August 2013, the US Department of Energy (DOE) Office of Science approved the project baseline and start of civil construction (CD2-3a) with a total project cost of \$730M, funded by DOE, MSU and the State of Michigan. FRIB obtained CD-3b approval from DOE in August 2014, and technical construction began in October 2014. The FRIB linac design has been developed and optimized through several iterations [2-6], with the goal of minimizing the overall project cost while maintaining the design performance and upgrade potential.

Figure 1 shows a schematic of the driver linac, which includes three linac segments with 44 accelerating modules and 2 folding segments with 4 matching cryomodules. The FRIB resonators are optimized for 4 different velocities:  $\beta = v/c = 0.041, 0.085, 0.29, \text{ and } 0.53$ . Quarter-wave resonators (QWRs) at 80.5 MHz are used for low velocities and half-wave resonators (HWRs) are used for medium velocities. The cryomodules contain superconducting resonators and superconducting solenoids with a peak field of 8 T for transverse focusing. The solenoids include dipole windings

for horizontal and vertical steering. The low- $\beta$  cryomodules include beam position monitors (BPMs). The cryomodule element counts are listed in Table 1. At completion, FRIB will be one-of-a-kind large scale low-beta and medium-beta superconducting linac.

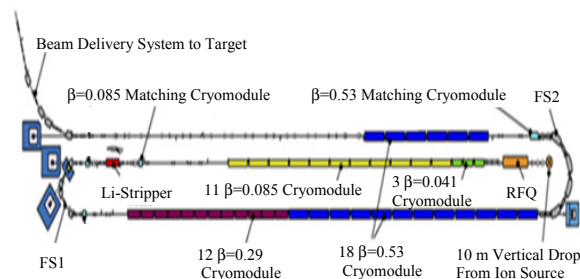


Figure 1: FRIB driver linac. The beam is produced in an ion source (orange), with the first stage of acceleration done in a copper radio-frequency quadrupole (RFQ, orange). Then the beam travels through the SRF cryomodules. Charge stripping is done before the first folding segment (FS1) to improve the acceleration efficiency.

### FRIB CRYOMODULE DESIGN

As shown in Figure 2, the FRIB cryomodules consist of a cold mass, baseplate, cryogenic system, thermal shield, magnetic shield, and vacuum vessel. This modular design allows us to use the same construction sequence for all 6 cryomodule types. The design introduces the innovation of a “bottom-up” assembly starting with the baseplate and ending with the installation of the vacuum vessel from the top. The bottom-up approach is different from the more traditional “top-down” approach, in which the cold mass is suspended from a top plate and lowered into a vacuum vessel. The bottom-up design, along with a carefully-engineered kinematic support system, ensures the placement of cavities and solenoids within alignment tolerance, without an actual alignment step, which tremendously reduces the cryomodule assembly time. This design concept was validated with an Engineering Test Cryomodule ETCM [7, 8]. The FRIB cryomodule design also adopted a U-tube interface with cryo-distribution developed by Jefferson Laboratory (JLab) for cryomodules at CEBAF and the Spallation

\* Work supported by the U.S. Department of Energy Office of Science under Cooperative Agreement DE-SC0000661

<sup>†</sup>xuti@frib.msu.edu

Table 1: FRIB Linac Cryomodules and their Contents

Cryomodule		$\beta$	Resonator		Solenoid		Cold BPM
Type	Quantity		Type	Quantity	Length (m)	Quantity	Quantity
Accelerating	3	0.041	QWR	12	0.25	6	6
Accelerating	11	0.085	QWR	88	0.50	33	33
Matching	1	0.085	QWR	4	-	0	0
Accelerating	12	0.29	HWR	72	0.50	12	0
Accelerating	18	0.53	HWR	144	0.50	18	0
Matching	1	0.53	HWR	4	-	0	0
Totals	46			324		69	39

Neutron Source (SNS). The U-tube design allows a cryomodule to be installed into and removed from the linac tunnel independently for service and maintenance. Years of operational experience with the CEBAF and SNS superconducting linacs have shown that this flexibility is essential to reliable operation for large-scale SRF accelerators. The cryogenic system is built onto the baseplate and hangs under the vacuum vessel after the cryomodule is completed, while the cold mass is supported by G-10 posts on top of the baseplate. This arrangement decouples the cavity string from the cryogenic system, which minimizes the risk of microphonics. This is especially important with QWRs, which are more susceptible to microphonics.

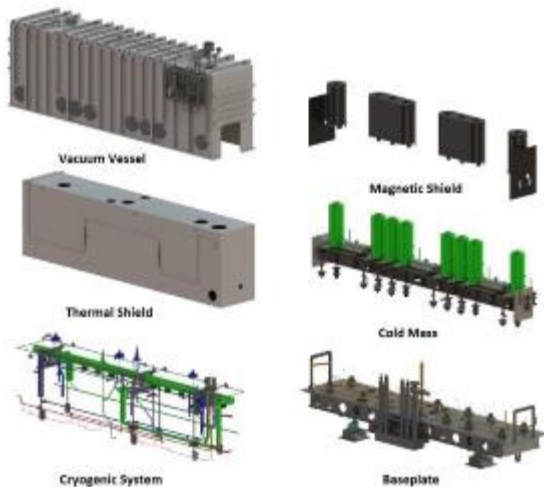


Figure 2: Exploded view of the subsystems for the FRIB  $\beta=0.085$  accelerating cryomodule.

### Cold Mass

Figure 3 shows the 6 cold mass types for the FRIB cryomodules. The cold mass design utilizes common end assemblies and integrated cooling channels close to the top flange and bottom flanges. The alignment rails are divided into segments as needed to limit the overall length. The segmentation makes them less sensitive to twist, easier to manufacture, and easier to handle in the clean room. For example, the  $\beta=0.085$  rail is separated into 3 segments, while the  $\beta=0.041$  rail is one single unit. Each rail segment has a fixed point to interface with the baseplate, and all other optical elements are mounted on the cold rails with

precisely-machined interface features. The alignment rails are made of 316L stainless steel; the cavities' helium vessels are made of commercially pure grade 2 titanium. The thermal mismatch between the rail and the cavity is accommodated by fixing one side of mounting flange to the rail and allowing the other side of the mounting flange to slide, guided by a specially-designed linear bearing. This design ensures predictable and repeatable thermal contraction. The mounting interface for the solenoids includes a novel rail interface design to allow yaw adjustment, to ensure that the more stringent alignment requirements for the magnets can be met. Mechanical vibration simulations have been performed for the modular bottom up cryomodule configuration. The resonator's first modal response occurs between 40 and 50 Hz for  $\beta=0.085$  cavities. Measurements have shown that the modular bottom-up design and kinematic cold mass support system adds little amplification to low-order modes [9].

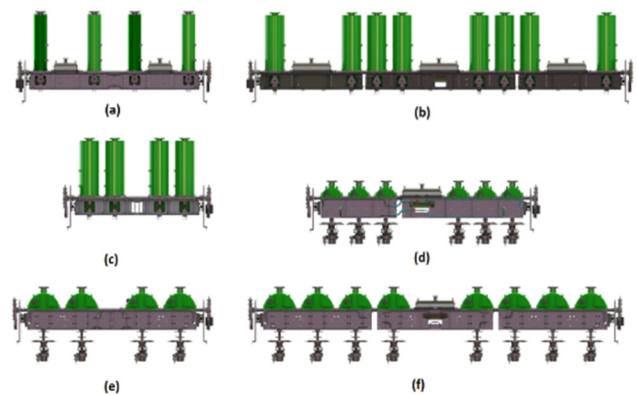


Figure 3: Side view of the cold masses for the FRIB cryomodules. (a)  $\beta=0.041$  accelerating, (b)  $\beta=0.085$  accelerating (3-segment rail), (c)  $\beta=0.085$  matching, (d)  $\beta=0.29$  accelerating (2-segment rail), (e)  $\beta=0.53$  matching, (f)  $\beta=0.53$  accelerating (3-segment rail).

### Baseplate and Alignment

Beam dynamics considerations are the basis for the alignment tolerances for the linac elements. The design of the baseplate is essential to the alignment. The assembly of the vacuum vessel to the baseplate makes the cryomodule a rigid and stable body. Both the baseplate and the vacuum vessel are made of A36 steel. Two rows of dowel holes are

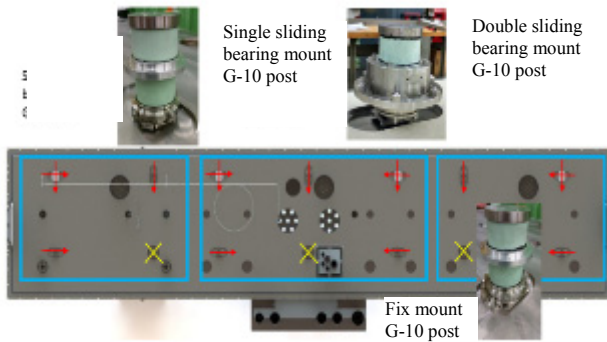


Figure 4: Cold mass support scheme for the  $\beta=0.085$  baseplate. Yellow X: fix post locations; red arrows: sliding post locations with contraction direction indicated.

machined precisely into the baseplate, on the master side (fixed) and the slave side (sliding), to interface to the cold mass using G-10 posts, as shown in Figure 4. The final alignment tolerance is achieved by control stack up tolerance of the interface features on the baseplate, G-10 posts, and alignment rail. The transverse placement is reached by the master side feature for each rail segment and the repeatable thermal contraction of the components; the slave side moves toward the master side during cool-down, as shown Figure 4. Surveys on the first two  $\beta=0.085$  cryomodules confirmed that a transverse alignment within 0.5 mm can be achieved during warm fabrication and assembly. The shift during cool down is repeatable within 0.33 mm of the calculated values, based on measurements on the FRIB prototype cryomodule with a wire position monitor (WPM) [7]. Hence the total alignment error is within the FRIB requirements without post-assembly adjustments (which would require additional work of up to a few weeks). This is one important advantage of the bottom-up cryomodule design.

### Cryogenics System

FRIB is the first large-scale low- $\beta$  linac with 4 types of cavities operating at 2 K. Figure 5 shows a simplified schematic of the cryogenic system for the  $\beta=0.085$  cryomodule. The cryomodule interfaces to the cryo-distribution system via a bayonet box for normal process lines and a warm manifold for utility modes (warm-up and cool-down) and relief stack. Each cryomodule can be cooled down and warmed up independently. The design is highly integrated with the cryogenic system and incorporates operational experience with the CEBAF and SNS cryomodules.

As can be seen in Figure 5, there are two primary circuits, 2 K (green) and 4 K (blue), which are controlled separately. The cryogenic system provides supercritical helium (3 bars, 4.5 K) to the 4 K and 2 K circuits in parallel, through two Joule-Thomson (JT) valves. The 4 K circuit provides cooling to the solenoids, alignment rail, and mechanical structure thermal intercept to minimize the 2 K static heat load. Taking advantage of the 4 K operation of the magnets, we use vapor-cooled current leads to minimize the 4 K heat load. In-house design and fabrication of the current leads provides a very cost effective solution.

The 2 K circuit adopts the SNS cryomodule design to include a 2 K/4 K heat exchanger inside the cryomodule to recover the cooling power from the 2 K return flow and improve 2 K efficiency. Instead of using a brazed aluminium plate-fin heat exchanger (BAHX) as was done in the SNS cryomodule, special finned tube heat exchangers were designed for FRIB by the JLab cryogenics group. Two different sizes are optimized to cover a wide range of 2 K heat loads and accommodate the different cryomodule types. The design is cost-effective and only a fraction of the corresponding BAHX type. The single-flow-path design ensures an even flow distribution over a wide range of flow conditions and maintains high performance. The thermal shield is made of 1100-H14 aluminium alloy panels for better thermal conductivity, with a 6061-T6 frame. The shield cooling channels are  $\Omega$ -shaped extruded tube (6063 T5 aluminium), stitch welded to the thermal shield after final assembly at FRIB. The 50 K circuit cools the thermal shield and the fundamental power couplers (FPCs) for the cavities.

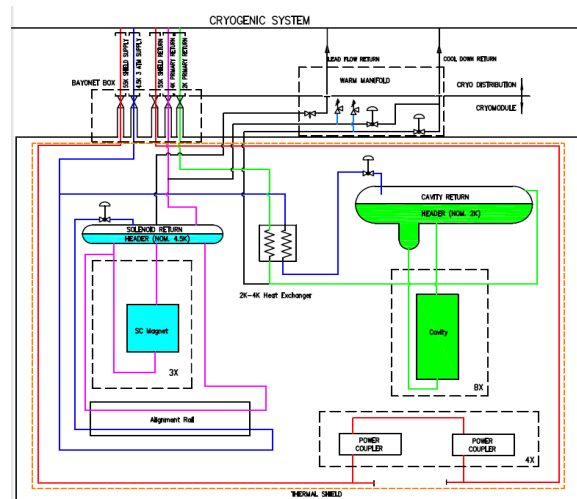


Figure 5: Simplified diagram of the cryogenic system for the  $\beta=0.085$  cryomodule. Blue: primary helium supply; cyan: 4 K circuit; green: 2 K circuit; red: shield circuit.

### Magnetic Shielding

In order to minimize the residual resistance due to the external magnetostatic field, the FRIB requirement is a field of <15 milligauss at the cavity surface for both the QWR and HWR when they transition from a normal to a superconductor. The magnetic shielding for the FRIB cryomodules includes bucking coils in the superconducting magnet packages and mu-metal shields around the cavities



Figure 6: Magnetic shields for (a) the  $\beta=0.085$  cryomodule, (b) the  $\beta=0.53$  cryomodule.

(Figure 6). Compared with a “global” shield around the entire cold mass, local shields only around the cavities are easier to assemble and more cost-effective. Moreover, local shielding makes the resonators less susceptible to possible magnetization of the cryomodule components. The thickness of the mu-metal layer is 1 mm for the QWRs and 2 mm for the HWRs; for these thicknesses, the critical mu-metal permeability to meet the specification is  $<10000$ . This requirement allows us to use commercially-available mu-metal. Cold tests on the first FRIB QWR cryomodule in 2016 confirmed that the magnetic shielding is adequate [10].

## CRYOMODULE PRODUCTION

### Infrastructure

Critical SRF tasks are done by FRIB in-house, including cavity etching, high-pressure water rinsing, clean room assembly, cavity certification testing, and cold mass assembly. Over 40 000 ft<sup>2</sup> on-site facilities (Figure 7), including



(a) Clean room



(b) Chemistry room



(c) Dewar test area



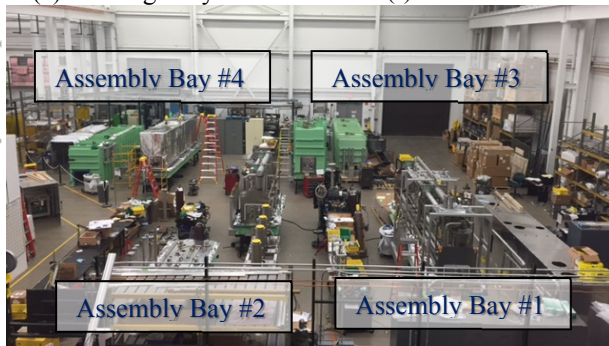
(d) Vacuum furnace



(e) SRF high bay test bunker



(f) EHB test bunker



(g) EHB cryomodule assembly area

a new building (the SRF high bay) with SRF infrastructure, are dedicated for cold mass and cryomodule assembly [11, 12]. The infrastructure is designed for delivery of 1.5 cold masses and 1.5 cryomodules per month at the peak of FRIB production. The 4000 ft<sup>2</sup> clean room, the custom-designed chemical etching facility tailored for FRIB cavity processing, the Coordinate Measuring Machine (CMM) inspection station, and the vacuum furnace for hydrogen degassing were completed by the end of 2014. A dedicated 900 W refrigerator with distribution box and 5000 liter storage Dewar support the cavity and cryomodule certification tests. Shown in Fig. 7c, the Dewar test area has been commissioned in 2015 and hosted over 100 cold tests since then. It has 2 independent test systems and can be expanded to 4 test pits if needed [13]. A robotic high pressure water rinse (HPWR) system has been commissioned in early 2016 for more efficient cavity surface preparation and reduce the human footprint in the clean room [14].

Two test bunkers are planned to support FRIB cryomodule cold tests. Bunker #1 is in operation and located in the NSCL east high bay (EHB), as shown in Figure 7f; Bunker #2, in the SRF high bay (Figure 7e), is currently being commissioned. The cryogenic distribution in Bunker #1 is the prototype transfer line for the linac tunnel. Therefore, the tests are done under realistic conditions. Operation at 2 K is done via a 2 g/s warm pump. Currently there are RF systems (4 kW, 80.5 MHz amplifier, LLRF system) for 2 cavities and magnet power supplies for one solenoid package. The control system uses dedicated PLC and IOC with EPICS. The Human Machine Interface (HMI) screens for control and testing are made in Control System Studio (CSS). The PPS has its own PLC interlocked with the RF amplifiers. Bunker #1 was commissioned at the end of 2014 and used for testing a FRIB QWR prototype cryomodule and the first two QWR production cryomodules successfully. Bunker #2 will be used to test the preproduction  $\beta=0.53$  HWR cryomodule.

### Cavity and Cold Mass Production

To date, FRIB has received over 120 vendor-produced cavities across all four types, which is  $>30\%$  of the total cavities needed for the FRIB linac. About half of the cavities have been processed and certified for cold mass installation. Processing and testing of the remaining cavities is in progress. The rework rate is about 17%, which is below the anticipated maximum rate. Some of rework effort is due to a lack of statistics on the frequency shift during cavity preparation steps, which is a one-time learning investment. Therefore, the rework rate is expected to decrease as the production work progresses. Figure 8 summarizes the present status of in-house cavity production work. Only a few cavities have not been certified due to field emission and frequency issues; 94% of the tested cavities are certified with a comfortable margin in  $Q$  and gradient [13].

Cold mass production has been progressing well (Figure 9). A total of 7 cold masses of 3 different types have been completed [15, 16]. Standard procedures and routers have been developed for the in-house work. The first full-size  $\beta=0.085$  cold mass was assembled in 1 month, well in

Figure 7: Cryomodule production infrastructure.

line with expectations. The cold tests on both the prototype cryomodule and the first production module showed no degradation in cavity quality factor ( $Q$ ) compared to vertical test results and no field emission at low field level, which showed that the preparation procedures and practices are sound, including cavity assembly, coupler installation, beam line component cleaning and installation, and pump down and back fill procedures.

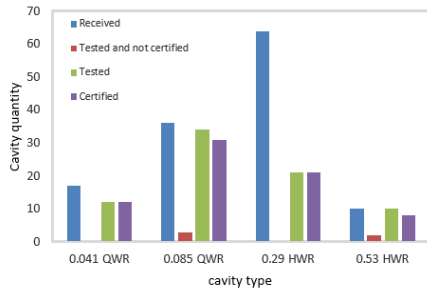


Figure 8: FRIB cavity production status (as of Sep 2016).

### Cryomodule Production and Testing

Currently, the cryomodule assembly area is located in the East High Bay of the existing NSCL building. Four assembly bays are in use to meet FRIB production requirements (Figure 7g). Because of the sequence of the bottom-up assembly, it is better for the cryomodule to be stationary for the entire assembly, rather than moving the cryomodules through specialized stations for different assembly steps. Hence, every bay is designed to be compatible with every cryomodule type.



(a)  $\beta=0.085$  cryomodule at assembly stage 4



(b)  $\beta=0.041$  cold mass and cryomodule at stage 5



(c)  $\beta=0.53$  cryomodule at assembly stage 4

Figure 9: Cryomodules in different production stages.

The modular cryomodule design allows for most of the components to be procured from outside vendors. This reduced in-house labor and streamlines the assembly work. The modular approach allows for a significant number of components to be common across different cryomodules, which simplifies the procurements, reduces the inventory, and facilitates the assembly work. The assembly work proceeds through 6 major stages: (1) assemble baseplate and bottom cryogenics; (2) install cold mass onto baseplate; (3) survey the alignment; (4) install the cryogenic system and magnet shielding; (5) install the thermal shield and multi-layer insulation; (6) attach the vacuum vessel and external components. After each stage, quality assurance and engineering inspections and approvals are required.

FRIB cryomodule production started in the second half of 2015, following the successful assembly and cold test of the prototype cryomodule. The first production cryomodule ( $\beta = 0.085$ , Figure 9a) was finished at the end of 2015. It was completed 6 weeks after receipt of the cold mass. Planned peak production rate can be achieved with 4 assembly bays staged and loaded to support the cryomodule mass production schedule as shown in Fig. 10. A second  $\beta = 0.085$  cryomodule and the first  $\beta = 0.041$  cryomodule have since been completed and the first two  $\beta = 0.085$  cryomodule have been cold tested and certified successfully. Cavity performance is consistent with Dewar test results in both cryomodules tests and no performance degradation is observed. The 2 K dynamic loads are 60% of the FRIB design goal. The bandwidth of the FPCs range from 26 Hz to 41 Hz. All cavities were locked at 6.1 MV/m (FRIB goal = 5.6 MV/m) within the phase and amplitude specification (2% peak-to-peak and 0.25 % RMS), even though the environment ground noise is higher than in the FRIB tunnel. The solenoids reached full field at 8 T without training quenches. Currently, four cryomodules (three different types) are being assembled, as seen in Figure 7g. The pre-production  $\beta=0.53$  cryomodule (CM501, Figure 9c) will be ready for testing by the end of September 2016.

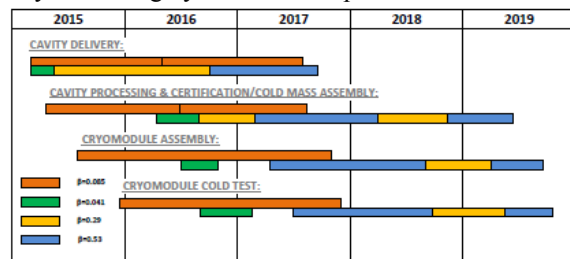


Figure 10: FRIB cryomodule production schedule.

### CONCLUSION

Over a decade of SRF development at MSU provides a solid foundation for the construction of the FRIB superconducting linac. The SRF subsystems for the FRIB cryomodules are developed and validated. A state of art SRF facility is in operation at MSU since the end of 2014 to support FRIB cryomodule work. Cavity and cryomodule production are ramping up. FRIB will receive all of the cavities by the end of 2017 and assemble and cold test all of the cryomodules by the end of 2019.

## REFERENCES

- [1] J. Wei *et al.*, “FRIB Accelerator Status and Challenges,” in *Proc. 26th Linear Accelerator Conference*, Tel Aviv, Israel, 2012, p. 417-421.
- [2] X. Wu *et al.*, “End-to-end beam simulations for the MSU RIA Driver Linac,” in *Proc. 22th Linear Accelerator Conference*, Lubeck, Germany, Aug. 2004, p. 594-598.
- [3] Q. Zhao *et al.*, “End-to-end beam dynamics simulations of the ISF Driver Linac,” in *Proc. 22th Particle Accelerator Conference*, Albuquerque, USA, 2007, p. 1775-1777.
- [4] Q. Zhao *et al.*, “Beam dynamics studies for the FRIB Driver Linac,” in *Proc. 23th Particle Accelerator Conference*, Vancouver, BC, Canada, 2009, p. 3901-3903.
- [5] R. York *et al.*, “Beam Dynamics in the FRIB Linac,” in *Proc. 46th ICFA Advanced Beam Dynamics Workshop on High-Intensity and High-Brightness Hadron Beams*, Morschach, Switzerland, 2010, p. 319-323.
- [6] Z. Q. He *et al.*, “Beam Dynamics Optimization of FRIB Folding Segment 1 with Single-type Re-buncher Cryomodule,” in *Proc. 6th International Particle Accelerator Conference*, Richmond, USA, 2015, p. 4042-4044.
- [7] K. Saito *et al.*, “FRIB Project: Moving to Production Phase,” in *Proc. 17th International Conference on RF Superconductivity*, Whistler, Canada, 2015, p. 1-5.
- [8] S. J. Miller *et al.*, “Low-Beta Cryomodule Design Optimized for Large-Scale Linac Installations,” in *Proc. 16th International Conference on RF Superconductivity*, Paris, France, 2013, p. 825-829.
- [9] S. J. Miller *et al.*, “Construction and Performance of FRIB Quarter Wave Prototype,” in *Proc. 17th International Conference on RF Superconductivity*, Whistler, Canada, 2015, p. 1446-1452.
- [10] Z. Zheng *et al.*, “Cost reduction for FRIB Magnetic Shielding,” presented at *28th Linear Accelerator Conference*, East Lansing, USA, 2016, Paper THPRC021.
- [11] L. Popielarski *et al.*, “SRF Highbay Technical Infrastructure for FRIB Production at Michigan State University,” in *Proc. 27th Linear Accelerator Conference*, Geneva, Switzerland, 2014, p. 954-956.
- [12] L. Popielarski *et al.*, “Low-Beta SRF Cavity Processing and Testing Facility for the Facility for Rare Isotope Beams at Michigan State University,” in *Proc. 17th International Conference on RF Superconductivity*, Whistler, Canada, 2015, p. 597-601.
- [13] J. Popielarski *et al.*, “Cryogenic Testing of Production Coaxial Resonators and Cryomodules for the FRIB Linac,” presented at *28th Linear Accelerator Conference*, East Lansing, USA, 2016, Paper TUPLR034.
- [14] Malloch *et al.*, “Design and Implementation of an Automated High-Pressure Water Rinse System for FRIB SRF Cavity Processing,” presented at *28th Linear Accelerator Conference*, East Lansing, USA, 2016, Paper TUPRC024.
- [15] K. Elliott *et al.*, “First FRIB  $\beta=0.041$  Production Coldmass Build,” presented at *28th Linear Accelerator Conference*, East Lansing, USA, 2016, Paper TUPLR033.
- [16] D. Victory *et al.*, “First FRIB  $\beta=0.53$  Prototype Coldmass Build,” presented at *28th Linear Accelerator Conference*, East Lansing, USA, 2016, Paper TUPLR030.